

Cationic Unsymmetrical 1,4-Diazabutadiene Complexes of Platinum(II)

Paul J. Albietz, Jr., Kaiyuan Yang, Rene J. Lachicotte, and Richard Eisenberg*

Department of Chemistry, University of Rochester, Rochester, New York 14627

Received January 21, 2000

The synthesis of the silyl-protected 1,4-diazabutadiene ligands glyoxal-bis((2- α -triisopropylsiloxyethyl)-6-methylphenyl)diimine (**TIPS-6-MPD**) and glyoxal-bis((2- α -triisopropylsiloxyethyl)-4-methylphenyl)diimine (**TIPS-4-MPD**) and their subsequent reactions with *trans*-Pt(SMe₂)₂(Me)Cl to generate the corresponding complexes (TIPS-6-MPD)Pt(Me)Cl (**1a**) and (TIPS-4-MPD)Pt(Me)Cl (**1b**) are described. Cationic complexes of the type [(*N,N*-cholate)-Pt(Me)(L)]BF₄ (where L = solvent/olefin and *N,N*-cholate = **TIPS-6-MPD** and **TIPS-4-MPD**) are generated by the reaction of chloro methyl complexes **1a** and **1b** with AgBF₄ in the presence of L. Various exchange reactions were examined for [(TIPS-6-MPD)Pt(Me)(NCCH₃)]-BF₄ (**2a**), in which it was determined that the coordinated solvent reversibly exchanges with acrylonitrile, ethylene, fumaronitrile, *cis*-pentenenitrile, benzonitrile, dimethyl sulfide, and carbon monoxide to generate the corresponding cationic complexes **3–9**, respectively. Kinetics experiments under pseudo-first-order conditions using 10-, 20-, and 30-fold excesses of benzonitrile demonstrate that **2a** undergoes ligand exchange via an associative pathway with a bimolecular rate constant k_2 of $(3.2 \pm 2.0) \times 10^{-4} \text{ M}^{-1} \text{ s}^{-1}$. Complex **2a** was found to initiate the polymerization of various electron-rich monomers. A detailed analysis of the reaction demonstrates that the initiation is cationic in nature. The molecular structure of **TIPS-6-MPD** has been determined by a single-crystal X-ray diffraction analysis. The free ligand adopts an *s-trans* conformation with a planar N=C–C=N backbone.

Introduction

Over the past decade, a growing interest in the use of palladium and other late transition metal diaryldiazabutadiene (Ar₂DAB) complexes has developed due to their high activities as α -olefin polymerization catalysts. Some of the most noteworthy of the work regarding such systems has been reported by Brookhart^{1–3} and describes the employment of well-defined complexes with activities comparable to those of the more classical early transition metal polymerization catalysts. Use of Ar₂DAB molecules as ligands for these systems allows for flexibility regarding the kinds of polymers that can be generated, since the ortho alkyl groups on the arylimine moiety influence the structure of the resulting polymer. Furthermore, synthesis of the ligands is based on relatively cheap and readily available starting materials that allow for a great deal of synthetic versatility at low cost.

Stimulated by the growing interest in palladium Ar₂DAB complexes as polymerization catalysts, the study of analogous electrophilic platinum complexes has also increased. Because of their greater stability, these platinum complexes constitute excellent model compounds for the more reactive Pd congeners.^{4–14} For

example, Ruffo et al.^{10–14} have recently reported the examination of a number of cationic platinum olefin complexes containing various ortho alkyl-substituted Ar₂DAB ligands. Successful structural characterization of two of these platinum–olefin complexes has been achieved, one in which a crystal structure of an η^2 -bound ethylene adduct was determined, and the other in which connectivity of an η^2 -bound methyl acrylate complex was established. Research on these Pt model compounds provides insight as to how olefins bind and interact with late transition metals, which in turn may then be applied to the design of future catalysts to increase their effectiveness and the types of polymers they can generate.

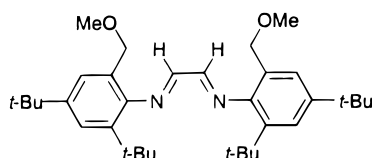
The use of electrophilic platinum complexes for C–H bond activation has also grown over the past few years.

- (5) van Asselt, R.; Elsevier, C. J.; Smeets, W. J. J.; Spek, A. L. *Inorg. Chem.* **1994**, *33*, 1521–1531.
- (6) van Asselt, R.; Elsevier, C. J.; Amatore, C.; Jutand, A. *Organometallics* **1997**, *16*, 317–328.
- (7) Albietz, P. J., Jr.; Yang, K.; Eisenberg, R. *Organometallics* **1999**, *18*, 2747–2749.
- (8) Yang, K.; Lachicotte, R. J.; Eisenberg, R. *Organometallics* **1997**, *16*, 5234–5243.
- (9) Yang, K.; Lachicotte, R. J.; Eisenberg, R. *Organometallics* **1998**, *17*, 5102–5113.
- (10) Ferrara, M. L.; Orabona, I.; Ruffo, F.; Funicello, M.; Panunzi, A. *Organometallics* **1998**, *17*, 3832–3834.
- (11) Ferrara, M. L.; Giordano, F.; Orabona, I.; Panunzi, A.; Ruffo, F. *Eur. J. Inorg. Chem.* **1999**, *1*, 1939–1947.
- (12) Fusto, M.; Giordano, F.; Orabona, I.; Ruffo, F. *Organometallics* **1997**, *16*, 5981–5987.
- (13) Ganis, P.; Orabona, I.; Ruffo, F.; Vitagliano, A. *Organometallics* **1998**, *17*, 2646–2650.
- (14) Zuccaccia, C.; Macchioni, A.; Orabona, I.; Ruffo, F. *Organometallics* **1999**, *18*, 4367–4372.

- (1) Killian, C. M.; Johnson, L. K.; Brookhart, M. *Organometallics* **1997**, *16*, 2005–2007.
- (2) Killian, C. M.; Tempel, D. J.; Johnson, L. K.; Brookhart, M. *J. Am. Chem. Soc.* **1996**, *118*, 11664–11665.
- (3) Johnson, L. K.; Killian, C. M.; Brookhart, M. *J. Am. Chem. Soc.* **1995**, *117*, 6414–6415.
- (4) van Asselt, R.; Rijnberg, E.; Elsevier, C. J. *Organometallics* **1994**, *13*, 706–720.

Bercaw,^{15–19} Periana,²⁰ Goldberg,²¹ and Tilset²² have recently reported a number of cationic Pt(II) complexes that undergo the intermolecular C–H bond cleavage of various substrates. Knowledge gained from these studies builds upon the seminal work of Shilov^{23,24} and may allow for the catalytic activation and subsequent functionalization of one of the most unreactive bonds in organic molecules. The observation that cationic Pt(II) complexes can activate these bonds demonstrates that a rich field of electrophilic chemistry exists for these complexes.

Recently we reported^{8,9} the synthesis and characterization of a series of Pd(II) and Pt(II) complexes coordinated to a new unsymmetrical 1,4-diazabutadiene ligand, **MOM-4,6-DBPD** (vide infra). The different ortho substituents on each aromatic ring result in a ligand that may potentially impose a C_2 symmetric environment on the coordinated metal ion. Although the ligand synthesis is both versatile and straightforward, it does entail a somewhat lengthy five-step procedure. Additionally, the presence of the bulky ortho substituents led to formation of two isolable but hard to separate isomers (syn and anti) upon complexation that differ in the relative orientation of the ortho *tert*-butyl and methoxymethyl (MOM) groups with respect to the coordination plane. Therefore, other routes to potentially C_2 symmetric Ar₂DAB derivatives have been examined.



MOM-4,6-DBPD

Herein we report on the two-step synthesis of two unsymmetrical Ar₂DAB ligands that are based on readily available starting materials and the synthesis, characterization, and reactivity of the corresponding cationic Pt(II) diimine complexes. A kinetics analysis for ligand exchange of one of the complexes has been conducted to establish the pathway by which displacement occurs. In this study we also describe the extraordinary ability of a cationic acetonitrile complex containing one of the Ar₂DAB ligands to polymerize various electron-rich olefins by a cationic mechanism. Part of this work has appeared in preliminary form.⁷

(15) Holtcamp, M. W.; Neling, L. M.; Day, M. W.; Labinger, J. A.; Bercaw, J. E. *Inorg. Chim. Acta* **1998**, *270*, 467–478.

(16) Holtcamp, M. W.; Labinger, J. A.; Bercaw, J. E. *J. Am. Chem. Soc.* **1997**, *119*, 848–849.

(17) Holtcamp, M. W.; Labinger, J. A.; Bercaw, J. E. *Inorg. Chim. Acta* **1997**, *265*, 117–125.

(18) Luinstra, G. A.; Wang, L.; Stahl, S. S.; Labinger, J. A.; Bercaw, J. E. *J. Organomet. Chem.* **1995**, *504*, 75–91.

(19) Stahl, S. S.; Labinger, J. A.; Bercaw, J. E. *J. Am. Chem. Soc.* **1996**, *118*, 5961–5976.

(20) Periana, R. A.; Taube, D. J.; Gamble, S.; Taube, H.; Satoh, T.; Fujii, H. *Science* **1998**, *280*, 560–564.

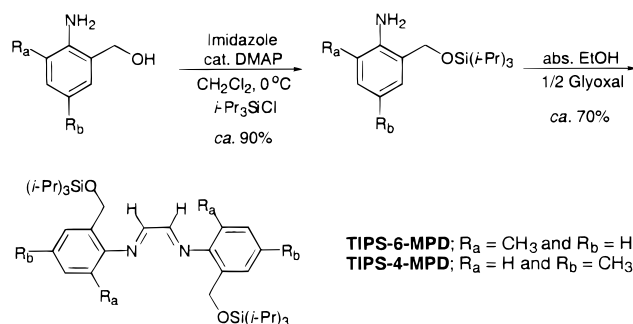
(21) Wick, D. D.; Goldberg, K. I. *J. Am. Chem. Soc.* **1997**, *119*, 10235–10236.

(22) Johansson, L.; Ryan, O. B.; Tilset, M. *J. Am. Chem. Soc.* **1999**, *121*, 1974–1975.

(23) Goldshleger, N. F.; Eskova, V. V.; Shilov, A. E.; Shteinmann, A. A. *Zh. Fiz. Khim.* **1972**, *46*, 1353.

(24) Kushch, K. A.; Lavrushko, V. V.; Misharin, Y. S.; Moravsky, A. P.; Shilov, A. E. *New J. Chem.* **1993**, *7*, 729.

Scheme 1



Results and Discussion

Synthesis of the Silyl-Protected Diimine Ligands.

Through the use of the commercially available 3- and 5-methyl-2-aminobenzyl alcohols, a two-step synthesis of potentially C_2 symmetric Ar₂DAB ligands was devised as shown in Scheme 1. It was found that silylation of the alcohol functionality was first necessary in order to synthesize the desired Ar₂DAB ligands and prevent oxazole formation by cyclization.²⁵ This was accomplished in high yields through the use of standard conditions (Scheme 1). A dichloromethane solution of the methyl-2-aminobenzyl alcohol, imidazole, and a catalytic amount of 4-(dimethylamino)pyridine (DMAP) in dichloromethane was cooled to 0 °C followed by the addition of triisopropylchlorosilane (TIPSCl) to result in the formation of the imidazole–hydrochloride salt as a white solid. After subsequent workup, the silyl-protected products were obtained in ca. 90% yield as pale, yellow oils.

As shown in Scheme 1, reaction of the silyl-ether derivatives of the methyl-2-aminobenzyl alcohols with 0.5 equiv of glyoxal generates the diazabutadiene ligands **TIPS-6-MPD** and **TIPS-4-MPD** as yellow solids with yields close to 70%. Both of the ligands demonstrate high solubilities in most organic solvents and can be recrystallized from CH₂Cl₂/ethanol (1:5 v/v) at –10 °C.

In the ¹H NMR spectrum of **TIPS-6-MPD** in CDCl₃, the characteristic imine resonance is observed as a singlet at δ 8.14. Likewise, the benzylic and methyl resonances are also singlets at δ 4.66 and 2.19, respectively, indicating effective mirror symmetry for the molecule. Coupling of the terminal methyl groups on the triisopropylsiloxy group to the proton on the secondary carbon results in splitting of the methyl resonance into a doublet at δ 1.08 (³J_{HH} = 6.4 Hz) and splitting of the methine proton into a septet at δ 1.14.

Due to the symmetry of the molecule, the ¹³C{¹H} NMR spectrum of **TIPS-6-MPD** is relatively simple. A

(25) The product is a white solid that precipitates out of the reaction mixture and is soluble in CH₂Cl₂, CHCl₃, acetone, and THF and insoluble in hexanes. The ¹H NMR spectrum and the elemental analysis of the compound are consistent with the structure drawn below. ¹H NMR (CDCl₃): δ 6.99 (2H), 6.79 (4H), 5.08 (1H), 5.05 (1H), 4.93 (2H), 4.90 (1H), 4.78 (1H), 4.21 (2H), 2.17 (3H), 2.16 (3H). Anal. Calcd for (C₁₈H₂₀N₂O₂): C, 72.95; H, 6.80; N, 9.45. Found: C, 73.07; H, 6.83; N, 9.41. Mp: 170 °C dec.

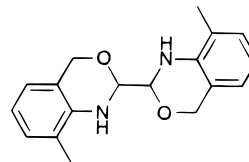


Table 1. Selected ^1H NMR Spectral Data for Major Isomers of New Compounds

compound	^1H NMR (δ) ^a
TIPS-6-MPD	8.14 (s, 1H, NCH), 7.49 (d, 1H, $^3J_{\text{HH}} = 7.1$ Hz, C ₆ H), 7.18–7.12 (m, 2H, C ₆ H), 4.66 (s, 2H, CH ₂), 2.19 (s, 3H, C ₆ H ₃ CH ₃), 1.14 (sep, 1H, Si(CH(CH ₃) ₂) ₃), 1.08 (d, 9 H, $^3J_{\text{HH}} = 6.4$ Hz, Si(CH(CH ₃) ₂) ₃)
TIPS-4-MPD	8.26 (s, 1H, NCH), 7.47 (s, 1H, C ₆ H), 7.07 (d, 1H, $J_{\text{ortho}} = 8.0$ Hz, C ₆ H), 6.92 (d, 1H, $J_{\text{ortho}} = 8.0$ Hz, C ₆ H), 4.95 (s, 2H, CH ₂), 2.38 (s, 3H, C ₆ H ₃ CH ₃), 1.17 (sep, 1H, Si(CH(CH ₃) ₂) ₃), 1.08 (d, 9 H, $^3J_{\text{HH}} = 6.7$ Hz, Si(CH(CH ₃) ₂) ₃)
1a	9.38 (s, 1H, $^3J_{\text{Pt-H}} = 104$ Hz, NCH), 8.81 (s, 1H, $^3J_{\text{Pt-H}} = 32$ Hz, NCH), 4.86 (d, 1H, $^2J_{\text{HH}} = 13$ Hz, CH ₂ H), 4.79 (d, 1H, $^2J_{\text{HH}} = 12$ Hz, CH ₂ H), 4.74 (d, 1H, $^2J_{\text{HH}} = 12$ Hz, CH ₂ H), 4.70 (d, 1H, $^2J_{\text{HH}} = 13$ Hz, CH ₂ H), 2.36 (s, 3H, C ₆ H ₃ CH ₃), 2.26 (s, 3H, C ₆ H ₃ CH ₃), 1.30 (s, 3H, $^2J_{\text{Pt-H}} = 80$ Hz, PtCH ₃)
1b	9.38 (s, 1H, $^3J_{\text{Pt-H}} = 98$ Hz, NCH), 8.85 (s, 1H, $^3J_{\text{Pt-H}} = 32$ Hz, NCH), 5.02 (d, 1H, $^2J_{\text{HH}} = 12$ Hz, CH ₂ H), 4.62–4.78 (m, 3H, CH ₂ H), 2.42 (s, 3H, C ₆ H ₃ CH ₃), 2.38 (s, 3H, C ₆ H ₃ CH ₃), 1.38 (s, 3H, $^2J_{\text{Pt-H}} = 80$ Hz, PtCH ₃)
2a	9.08 (s, 1H, NCH), 8.98 (s, 1H, NCH), 5.13 (d, 1H, $^2J_{\text{HH}} = 14$ Hz, CH ₂ H), 4.84 (d, 1H, $^2J_{\text{HH}} = 14$ Hz, CH ₂ H), 4.79 (d, 1H, $^2J_{\text{HH}} = 14$ Hz, CH ₂ H), 4.68 (d, 1H, $^2J_{\text{HH}} = 14$ Hz, CH ₂ H), 2.30 (s, 3H, C ₆ H ₃ CH ₃), 2.25 (s, 3H, C ₆ H ₃ CH ₃), 2.06 (s, 3H, CH ₂ CN), 0.73 (s, 3H, $^2J_{\text{Pt-H}} = 74$ Hz, PtCH ₃)
2b	9.08 (s, 1H, NCH), 8.95 (s, 1H, NCH), 5.27 (d, 1H, $^2J_{\text{HH}} = 13$ Hz, CH ₂ H), 4.93 (d, 1H, $^2J_{\text{HH}} = 13$ Hz, CH ₂ H), 4.82 (d, 1H, $^2J_{\text{HH}} = 13$ Hz, CH ₂ H), 4.73 (d, 1H, $^2J_{\text{HH}} = 13$ Hz, CH ₂ H), 2.43 (s, 3H, C ₆ H ₃ CH ₃), 2.40 (s, 3H, C ₆ H ₃ CH ₃), 2.21 (s, 3H, CH ₂ CN), 0.82 (s, 3H, $^2J_{\text{Pt-H}} = 74$ Hz, PtCH ₃)
3	9.12 (s, 1H, NCH), 9.01 (s, 1H, NCH), 6.27 (d, 1H, $^3J_{\text{cis}} = 12$ Hz, CH ₂ CHCN), 5.97 (d, 1H, $^3J_{\text{trans}} = 18$ Hz, CH ₂ CHCN), 5.52 (dd, 1H, $^3J_{\text{cis}} = 12$ Hz, $^3J_{\text{trans}} = 18$ Hz, CH ₂ CHCN), 2.31 (s, 3H, C ₆ H ₃ CH ₃), 2.24 (s, 3H, C ₆ H ₃ CH ₃), 0.74 (s, 3H, $^2J_{\text{Pt-H}} = 76$ Hz, PtCH ₃)
4	9.11 (s, 1H, NCH), 9.06 (s, 1H, NCH), 3.97 (m, 4H, $J_{\text{Pt-H}} \approx 64$ Hz, ethylene), 2.30 (s, 3H, C ₆ H ₃ CH ₃), 2.22 (s, 3H, C ₆ H ₃ CH ₃), 0.37 (s, 3H, $^2J_{\text{Pt-H}} = 68$ Hz, PtCH ₃)
5	9.12 (s, 1H, NCH), 8.95 (s, 1H, NCH), 6.20 (d, 1H, $^3J_{\text{trans}} = 16$ Hz, CNCHCHCN), 6.07 (d, 1H, $^3J_{\text{trans}} = 16$ Hz, CNCHCHCN), 2.30 (3H, C ₆ H ₃ CH ₃), 2.25 (s, 3H, C ₆ H ₃ CH ₃), 0.77 (s, 3H, $^2J_{\text{Pt-H}} = 72$ Hz, PtCH ₃)
6	9.09 (s, 1H, NCH), 9.03 (s, 1H, NCH), 6.68 (m, 1H, NCCHCHCH ₂ CH ₃), 5.25 (d, 1H, $^3J_{\text{HH}} = 11$ Hz, NCCHCHCH ₂ CH ₃), 2.32 (s, 3H, C ₆ H ₃ CH ₃), 2.24 (s, 3H, C ₆ H ₃ CH ₃), 1.90 (m, 2H, NCCHCHCH ₂ CH ₃), 0.95 (t, 3H, $^3J_{\text{HH}} = 7.4$ Hz, NCCHCHCH ₂ CH ₃), 0.74 (s, 3H, $^2J_{\text{Pt-H}} = 76$ Hz, PtCH ₃)
7	9.16 (s, 1H, NCH), 9.05 (s, 1H, NCH), 2.34 (s, 3H, C ₆ H ₃ CH ₃), 2.27 (s, 3H, C ₆ H ₃ CH ₃), 0.81 (s, 3H, $^2J_{\text{Pt-H}} = 70$ Hz, PtCH ₃)
8	9.14 (s, 1H, NCH), 9.08 (s, 1H, NCH), 2.61 (s, 3H, C ₆ H ₃ CH ₃), 2.23 (s, 3H, C ₆ H ₃ CH ₃), 2.06 (s, 6H, $^3J_{\text{Pt-H}} = 56$ Hz, S(CH ₃) ₂), 0.65 (s, 3H, $^2J_{\text{Pt-H}} = 74$ Hz, PtCH ₃)
9	9.22 (s, 1H, NCH), 9.09 (s, 1H, NCH), 2.39 (s, 3H, C ₆ H ₃ CH ₃), 2.26 (s, 3H, C ₆ H ₃ CH ₃), 0.80 (s, 3H, $^2J_{\text{Pt-H}} = 80$ Hz, PtCH ₃)

^a All ^1H NMR spectra were recorded in CDCl₃ solutions. Chemical shift values are reported in ppm. Abbreviations: br, broad; s, singlet; d, doublet; dd, doublet of doublets; m, multiplet; t, triplet; sep, septet.

Table 2. Selected $^{13}\text{C}\{^1\text{H}\}$ NMR Spectral Data for Major Isomers of New Compounds TIPS-6-MPD, TIPS-4-MPD, and 1–4

compound	$^{13}\text{C}\{^1\text{H}\}$ NMR (δ) ^a
TIPS-6-MPD	163.6 (NCCN), 61.6 (CH ₂), 18.8 (C ₆ H ₃ CH ₃), 18.1 (Si(CH(CH ₃) ₂) ₃), 12.0 (Si(CH(CH ₃) ₂) ₃)
TIPS-4-MPD	158.9 (NCCN), 61.3 (CH ₂), 21.4 (C ₆ H ₃ CH ₃), 18.1 (Si(CH(CH ₃) ₂) ₃), 12.1 (Si(CH(CH ₃) ₂) ₃)
1a	165.2 (NCCN), 164.1 (NCCN), 62.5 (CH ₂), 61.0 (CH ₂), –11.1 (PtCH ₃ , $J_{\text{Pt-C}} = 684$ Hz)
1b	165.2 (NCCN), 162.7 (NCCN), 62.9 (CH ₂), 61.4 (CH ₂), –10.2 (PtCH ₃ , $J_{\text{Pt-C}} = 706$ Hz)
2a	175.4 (NCCN), 166.5 (NCCN), 119.7 (CNCH ₃), 60.6 (CH ₂), 2.59 (CNCH ₃), –11.7 (PtCH ₃ , $J_{\text{Pt-C}} = 664$ Hz)
2b	173.9 (NCCN), 163.9 (NCCN), 120.0 (CNCH ₃), 61.3 (CH ₂), 60.9 (CH ₂), 3.73 (CNCH ₃), –11.2 (PtCH ₃ , $J_{\text{Pt-C}} = 670$ Hz)
3	176.0 (NCCN), 167.2 (NCCN), 142.3 (CH ₂ CHCN), 117.9 (CH ₂ CHCN), 104.8 (CH ₂ CHCN), 60.6 (CH ₂), 60.5 (CH ₂), –11.4 (PtCH ₃ , $J_{\text{Pt-C}} = 644$ Hz)
4^b	177.4 (NCCN), 169.7 (NCCN), 77.3 (ethylene, $J_{\text{Pt-C}} = 182$ Hz), 61.6 (CH ₂), 60.9 (CH ₂), –4.5 (PtCH ₃ , $J_{\text{Pt-C}} = 644$ Hz)

^a All $^{13}\text{C}\{^1\text{H}\}$ NMR spectra were recorded in CDCl₃ solutions. Chemical shift values are reported in ppm. ^b $^{13}\text{C}\{^1\text{H}\}$ NMR spectrum was recorded in CD₂Cl₂.

single resonance for the diimine carbon is observed at δ 163.6, and the benzylic carbon atom with the silyl-ether substituent resonates as a singlet at δ 61.6. The resonance of the methyl group carbon atoms ortho to the imine on the ring occur at δ 18.8, and two resonances for the TIPS group are seen at δ 18.1 and 12.0. Since the silyl-protected Ar₂DAB ligands and the corresponding platinum complexes demonstrate similar spectroscopic features, a detailed discussion of only one of the representative compounds in each section is necessary. Furthermore, complexes **1a**, **2a**, **3**, **4**, **5**, **6**, **7**, **8**, and **9** exist as two isomers (vide infra) that differ in orientation of the triisopropylsiloxy groups with respect to the coordination plane. In those sections, only the

resonances of the major isomer (ca. 80%) are discussed. Tables 1 and 2 summarize the results of ^1H and $^{13}\text{C}\{^1\text{H}\}$ NMR characterization of all of the compounds reported in this paper. Tables of the spectral data for the minor isomers **1a'**, **2a'**, **3'**, **4'**, **5'**, **6'**, **7'**, **8'**, and **9'** are contained within the Supporting Information.

A single-crystal X-ray diffraction analysis confirmed the identity of the ligand. Crystals of the ligand were grown from a concentrated solution of CH₂Cl₂/ethanol (1:4 v/v). The ORTEP diagram of **TIPS-6-MPD** is shown in Figure 1, with details of the structure determination shown in Table 3 and relevant bond distances and bond angles listed in Tables 4 and 5. As expected, **TIPS-6-MPD** adopts an s-trans orientation about the central

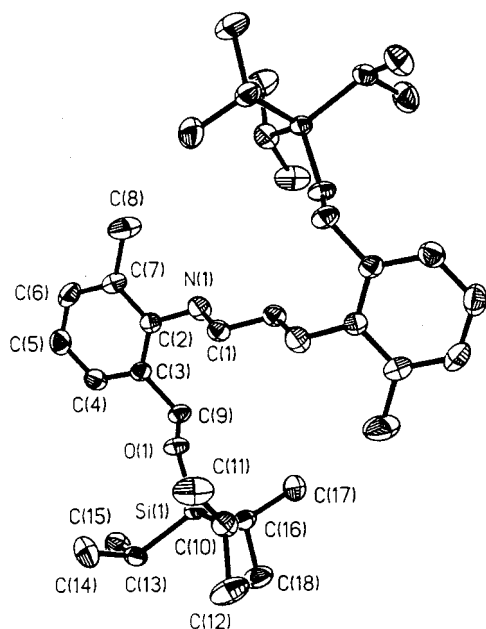


Figure 1. ORTEP diagram of **TIPS-6-MPD** shown in an *s-trans* orientation. Thermal ellipsoids are drawn at 30% probability. Hydrogen atoms are omitted for clarity.

Table 3. Summary of Crystallographic Data for TIPS-6-MPD

Crystal Parameters	
chemical formula	C ₃₆ H ₆₀ N ₂ O ₂ Si ₂
fw	609.04
cryst syst	triclinic
space group (no.)	P1
Z	1
a, Å ^a	8.1101(10)
b, Å	8.7180(2)
c, Å	13.2157(3)
α, deg	86.6100(10)
β, deg	78.6380(10)
γ, deg	87.3270(10)
volume, Å ³	913.90(3)
ρ _{calc} , g·cm ⁻³	1.107
cryst dimens, mm ⁻³	0.28 × 0.32 × 0.40
temp, °C	-80(2)
Measurement of Intensity Data and Refinement Parameters	
radiation (λ, Å)	Mo, Kα (0.71073)
2θ range, deg	3–57
total data	5682
no. of unique data	4021
R _{int} , R _{sigma} (%) ^b	1.18, 2.36
no. of obsd data (I > 2σ(I))	3622
no. of params varied	197
μ, mm ⁻¹	0.129
abs corr	empirical (SADABS) ^c
range of transmn factors	0.801–0.648
GOF ^d	1.066
R1(F _o), wR2(F _o ²) obsd (%) ^e	3.66, 10.45
R1(F _o), wR2(F _o ²) all (%)	4.03, 10.70

^a It has been noted that the integration program SAINT produces cell constant errors that are unreasonably small, since systematic error is not included. More reasonable errors might be estimated at 10× the listed value. ^b $R_{\text{int}} = \sum |F_o^2 - F_o^2(\text{mean})| / \sum |F_o^2|$; $R_{\text{sigma}} = \sum [\sigma(F_o^2)] / \sum |F_o^2|$. ^c The SADABS program is based on the method of Blessing; see Blessing, R. H. *Acta Crystallogr., Sect A* **1995**, 51, 33. ^d $\text{GOF} = [\sum [w(F_o^2 - F_c^2)^2] / (n - p)]^{1/2}$, where n and p denote the number of data and parameters. ^e $R1 = (\sum |F_o| - |F_c|) / \sum |F_o|$; $wR2 = [\sum [w(F_o^2 - F_c^2)^2] / \sum [w(F_o^2)^2]]^{1/2}$ where $w = 1/[\sigma^2(F_o^2) + (aP)^2 + bP]$ and $P = [\text{Max}(0, F_o^2) + 2F_c^2]/3$.

C–C bond in the backbone of the molecule. The molecule possesses a crystallographically imposed inversion center, and therefore the N=C–C=N portion of **TIPS-6-**

Table 4. Selected Bond Distances (Å) for TIPS-6-MPD

Si(1)–O(1)	1.656(1)	C(1)–C(1)′	1.463(2)
Si(1)–C(10)	1.880(11)	C(3)–C(9)	1.506(2)
O(1)–C(9)	1.423(1)	C(7)–C(8)	1.505(2)
N(1)–C(1)	1.256(2)	C(10)–C(11)	1.524(2)
N(1)–C(2)	1.420(2)		

Table 5. Selected Bond Angles (deg) for TIPS-6-MPD

O(1)–Si(1)–C(10)	104.99(6)	C(3)–C(2)–N(1)	123.04(11)
O(1)–Si(1)–C(13)	110.01(5)	C(7)–C(2)–N(1)	116.16(11)
C(10)–Si(1)–C(16)	111.74(6)	C(4)–C(3)–C(9)	118.93(11)
C(9)–O(1)–Si(1)	126.49(8)	C(2)–C(7)–C(8)	120.92(14)
C(1)–N(1)–C(2)	120.82(11)	O(1)–C(9)–C(3)	111.17(10)
N(1)–C(1)–C(1)′	120.49(14)	C(11)–C(10)–C(12)	110.10(13)
C(3)–C(2)–C(7)	120.55(12)	C(11)–C(10)–Si(1)	113.48(10)

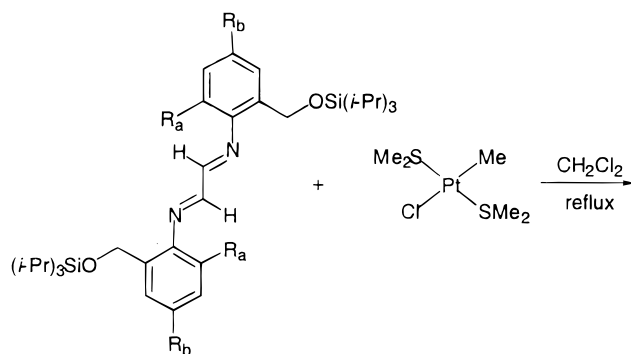
MPD is rigorously planar, with the triisopropylsiloxy-methyl substituents located on opposite sides of the Ar₂DAB backbone. Due to steric interactions between the silyl-ether substituents and the imine protons, the phenyl rings of the imine N atoms are tilted out of the plane of the N=C–C=N backbone, as indicated by the torsion angles of 123.55(0.14)° and -62.15(0.18)° for C(1)–N(1)–C(2)–C(7) and C(1)–N(1)–C(2)–C(3), respectively. The bond distances for the central C–C single bond in the backbone and the C=N double bond are 1.463(2) and 1.256(2) Å, respectively. These bond lengths are consistent with other structurally characterized diimines.^{8,26}

The 3- and 5-methyl-2-aminobenzyl alcohols differ only in the placement of the methyl substituent on the aromatic ring, which in turn leads to Ar₂DAB ligands having one or two ring substituents ortho to the imine N positions. Once the ligands are complexed to the metal, the presence of the second ortho substituent on the aryl-imine moiety has consequences regarding the ease of rotation about the N–C_(ipso) bond. Previous work has demonstrated⁹ that hindered rotation about this bond can result in two *isolable* isomers differing solely in the relative orientation of the pairs of ortho substituents with respect to the coordination plane. On the other hand, use of an Ar₂DAB ligand with only one ortho substituent leads to the synthesis of only a single product complex.

Synthesis of (N,N-chelate)Pt(Me)Cl, where N,N-chelate = TIPS-6-MPD and TIPS-4-MPD (1a and 1b). The reaction of the Ar₂DAB ligand **TIPS-6-MPD** or **TIPS-4-MPD** with *trans*-Pt(SMe₂)₂MeCl in refluxing dichloromethane proceeds smoothly to yield complexes **1a** and **1b**, respectively (eq 1). The two complexes are obtained as dark purple solids with isolated yields for this reaction in the 70–90% range. The complexes may be further purified by recrystallization from CH₂Cl₂/hexanes (1:4 v/v) at -35 °C. Complexes **1a** and **1b** are soluble in most organic solvents, especially in CH₂Cl₂ and CHCl₃, but are slightly less soluble in acetone, acetonitrile, benzene, and toluene. At low temperatures, the compounds are essentially insoluble in hydrocarbon solvents. Both of the platinum complexes are stable to air and moisture in both the solid state and in solution.

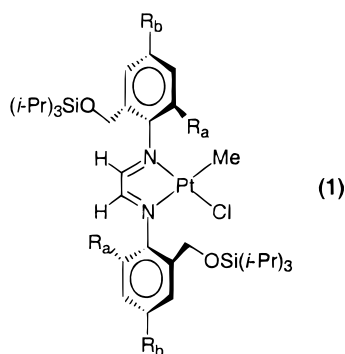
Characterization of **1a** and **1b** was accomplished by ¹H and ¹³C{¹H} NMR spectroscopies as well as by

(26) Van Koten, G.; Vrieze, K. *Adv. Organomet. Chem.* **1982**, 21, 151–239.



TIPS-6-MPD; $R_a = \text{CH}_3$ and $R_b = \text{H}$

TIPS-4-MPD; $R_a = \text{H}$ and $R_b = \text{CH}_3$



1a; $R_a = \text{CH}_3$ and $R_b = \text{H}$

1b; $R_a = \text{H}$ and $R_b = \text{CH}_3$

elemental analyses. In the ^1H NMR spectrum of complex **1a** in CDCl_3 , two resonances at δ 9.38 and 8.81 are observed that correspond to the imine protons on the backbone of the ligand. The resonances are shifted considerably downfield from those of the free ligand. The fact that there are two separate resonances provides evidence of the different ligands trans to the two coordinated imines of the **TIPS-6-MPD** ligand and the consequent asymmetry of **1a**. Both of the resonances show broad platinum satellites with coupling constants of 104 and 32 Hz, respectively. The smaller coupling constant for the latter resonance is due to weaker binding of the corresponding imine to platinum. Since the methyl group has a stronger trans-effect ligand than the chloride, this resonance most likely corresponds to the proton on the imino group trans to the methyl group. These observations are consistent with other characterized unsymmetrical chloro methyl complexes.¹² The breadth of the ^{195}Pt satellites is probably due to a contribution from chemical shift anisotropy (CSA). Work by Sadler et al.²⁷ in 1982 demonstrated that CSA increases the ^{195}Pt relaxation rate and broadens the satellites by acting as the dominant spin–lattice relaxation mechanism. Additionally, it was noted that broadening of the satellites is temperature dependent, with effects from CSA increasing as the temperature is lowered. The results from variable-temperature (VT) ^1H NMR experiments conducted on the chloro methyl complexes **1a** and **1b** are consistent with this notion. The satellites for the imine resonances of **1b** are not

observed at 198 K due to substantial broadening, while spectra obtained for complex **1a** show sharpening of the satellites as the temperature is increased from room temperature to 355 K. Similar effects are observed for the $\text{Pt}-\text{CH}_3$ group that resonates at δ 1.30 ($^2J_{\text{Pt}-\text{H}} = 80$ Hz) since the half-width $\Delta\nu_{1/2}$ for the platinum-methyl satellites of **1a** decreases from 11 Hz at room temperature to 6 Hz at 355 K.

In addition to the imine protons and the $\text{Pt}-\text{CH}_3$ group, four doublets in the range δ 4.70–4.86 ($^2J_{\text{HH}} \approx 13$ Hz) are observed that correspond to the benzylic protons bearing the silyl-ether substituents. These resonances demonstrate the diastereotopic nature of each pair of benzylic protons and are consistent with the AB coupling patterns observed for other geometrically rigid benzylic systems.^{8,9,28–30} All of the platinum complexes reported in this paper demonstrate similar sets of diastereotopic resonances.

The $^{13}\text{C}\{^1\text{H}\}$ NMR spectrum of **1a** shows two resonances for the diimine carbons at δ 165.2 and 164.1 consistent with the lower symmetry of the complex. Likewise, a set of 12 resonances corresponding to the phenyl carbons are found in the aromatic region of the spectrum (ca. δ 125), and two resonances at δ 62.5 and 61.0 are observed for the benzylic carbon atoms bearing the silyl-ether substituents. The $\text{Pt}-\text{CH}_3$ resonance is seen at δ –11.1 with $J_{\text{Pt}-\text{C}} = 684$ Hz.

The room-temperature ^1H and $^{13}\text{C}\{^1\text{H}\}$ NMR spectra of **1b** show that only one isomer exists in solution. In contrast, freshly recrystallized samples of **1a** contain a small amount (approximately 4%) of a second species. Due to the results reported previously for complexes of the much bulkier ligand system **MOM-4,6-DBPD**,^{8,9} the existence of syn and anti isomers of the MPD complexes was investigated. Low-temperature ^1H NMR spectral studies of complex **1b** proved to be quite informative. At 248 K, a considerable amount of broadening was observed in the benzylic region of the spectrum. At 223 K, decoalescence of the benzylic resonances was seen to occur, while the aromatic and imine resonances began to broaden. At 198 K, the slow exchange limit was reached as sharpened resonances for the syn and anti isomers of **1b** were observed. On the basis of the coalescence temperature (T_c) of the imine resonances, the ΔG^\ddagger value for interconversion between the two isomers of **1b** is estimated to be ca. 12 kcal/mol at 223 K.

When a toluene- d_8 solution of complex **1a** was allowed to stand at room temperature (296 K) for 3 days in a resealable NMR tube, the intensities of the resonances corresponding to the syn isomer of the complex (**1a'**) eventually increased. While less than 4% of the syn isomer was initially present, an equilibrium was established between the two isomers after 1 day. The equilibrium constant, K_{eq} , corresponding to [syn isomer]/[anti isomer], was estimated as 0.2, corresponding to ΔG° of ca. 1.0 kcal/mol for the equilibrium. Two conclusions regarding the aforementioned experiments may be made. For complex **1b**, rapid interconversion is occurring at room temperature since new resonances are observed to grow in when lower temperatures are

(28) Jennings, B. *Chem. Rev.* **1975**, *75*, 307.

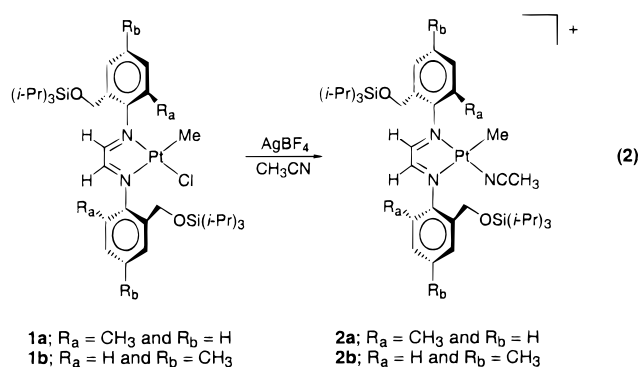
(29) Atwood, D. A.; Remington, M. P.; Rutherford, D. *Organometallics* **1996**, *15*, 4763–4769.

(30) Atwood, D. A.; Jegier, J. A.; Martin, K. J.; Rutherford, D. *Organometallics* **1995**, *14*, 1453–1460.

(27) Ismail, I. M.; Kerrison, S. J. S.; Sadler, P. J. *Polyhedron* **1982**, *1*, 57–59.

accessed. In contrast, it is evident that rapid interconversion does not occur for **1a**. The second ortho substituent on each aromatic ring of **1a** impedes interconversion between the isomers by making rotation about the N–C_(ipso) bond sterically encumbered. The results also suggest that interconversion does not proceed by prior dissociation of the imine N.

Generation of the Cationic Complex [(N,N-chelate)Pt(Me)(CH₃CN)]BF₄, Where N,N-chelate = TIPS-6-MPD and TIPS-4-MPD (2a** and **2b**) via Halide Abstraction.** The chloro methyl complexes serve as convenient precursors for the generation of cationic platinum complexes. The reaction between **1a** or **1b** and 1.06 equiv of AgBF₄ in acetonitrile (eq 2) at room temperature results in orange-colored solutions.



Following subsequent workup, the acetonitrile adducts **2a** and **2b** are isolated as orange solids in ca. 70% yield. The products are air- and moisture-stable both in the solid state and in solution and can be purified by recrystallization from CH₂Cl₂/hexanes (1:4 v/v) at –35 °C. The solvento complexes are soluble in acetonitrile, CH₂Cl₂, CHCl₃, THF, and acetone and insoluble in diethyl ether, benzene, toluene, and hexanes. Complexes **2a** and **2b** were characterized by ¹H and ¹³C{¹H} NMR spectroscopies as well as by elemental analyses. An X-ray diffraction analysis of **2a**, which has been described in the preliminary report on this study,⁷ shows the complex to have the expected square-planar coordination geometry with an anti conformation for the two (*i*-Pr)₃SiOCH₂ groups and a difference in Pt–N(imine) distances arising from the different trans ligands.

The ¹H NMR spectrum of **2a** in CDCl₃ revealed two singlets at δ 9.08 and 8.98 corresponding to the imine protons on the backbone of the ligand. A sharp singlet is observed at δ 2.06 for coordinated acetonitrile, even in the presence of free MeCN, indicating that any solvent exchange occurs slowly on the NMR time scale at ambient temperature (vide infra). The other characteristic feature of this complex is the resonance at δ 0.73 (²J_{Pt–H} = 74 Hz) assigned to the platinum-bound methyl group.

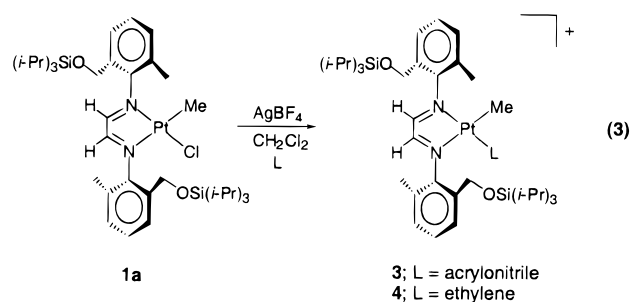
A ¹³C{¹H} NMR spectrum was obtained of the acetonitrile adduct **2a**. The observed resonances are very similar to those seen for the neutral chloro methyl complexes. The coordinated acetonitrile resonances are seen at δ 119.7 (CH₃CN) and 2.59 (CH₃CN) and were found to be consistent with other examples of cationic platinum acetonitrile complexes.⁹

As noted above, exchange between free and coordinated acetonitrile is slow on the NMR time scale since

averaging of the two resonances is not observed when free MeCN is present in solution. An upper limit on the rate of exchange at the coalescence temperature *T*_c (>333 K) in CDCl₃ can be estimated to be 71 s^{–1} based on the chemical shift difference between the free and coordinated acetonitrile resonances at the slow exchange limit. The actual coalescence temperature could not be determined due to the low boiling point of CDCl₃. In an attempt to verify that exchange of acetonitrile does occur, albeit slowly, a reaction of **2a** with CD₃CN was carried out in an NMR tube (Scheme 2). Complex **2a** was dissolved in CD₃CN and allowed to stand at room temperature for 1 h. After removal of the solvent, the residue was redissolved in CDCl₃ and the ¹H NMR spectrum was obtained. It was observed that the resonance for coordinated acetonitrile at δ 2.06 had disappeared, while the rest of the spectrum remained completely unchanged. In an analogous fashion, the reaction of **2a-d**₃ with CH₃CN regenerates **2a**.

For complex **2a**, two sets of resonances are seen in the ¹H NMR spectrum, indicating that two complexes are present in solution in an approximate 80:20 ratio. As was briefly mentioned in the beginning of this report, all of the TIPS-6-MPD complexes discussed in this paper exhibit two sets of resonances in roughly the same ratio. Given the observations of the related chloro methyl complex **1a**, the minor set of resonances is attributable to the syn isomer that forms through hindered rotation about the N–C_(ipso) bond. In contrast to **2a**, only one set of resonances is observed in the room-temperature ¹H NMR spectrum of **2b**. Absence of the ortho methyl groups allows free rotation to occur, resulting in a time-averaged spectrum of the syn and anti isomers. This is consistent with the variable-temperature NMR studies of the neutral chloro methyl complexes discussed in the previous section.

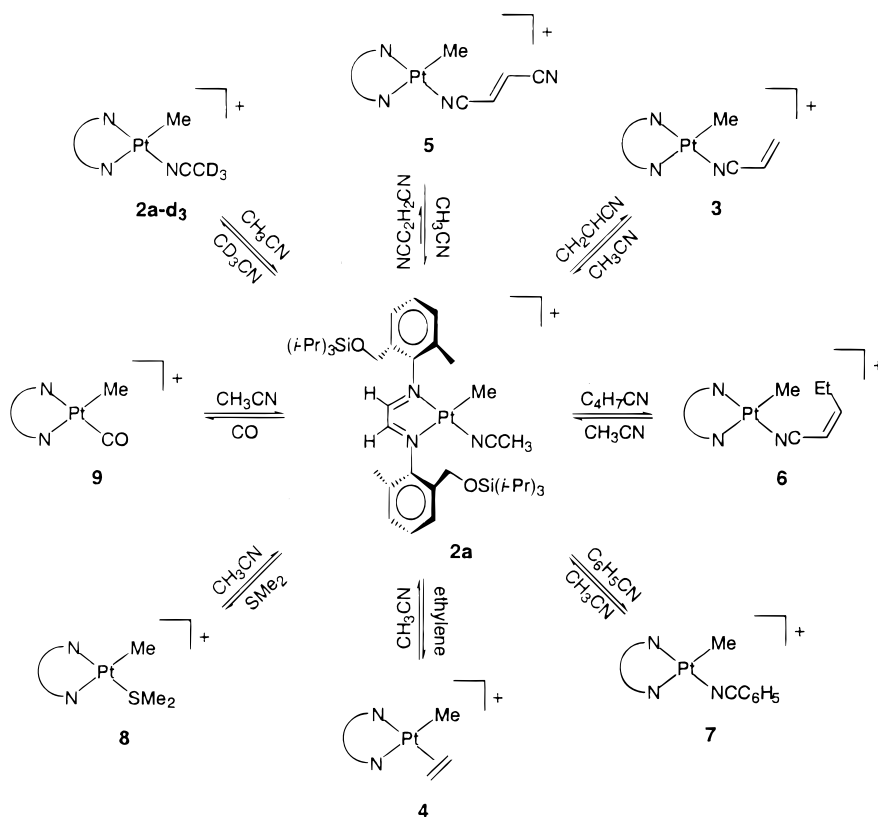
Synthesis of [(TIPS-6-MPD)Pt(Me)(CH₂CHCN)]BF₄ (3**).** Complex **3** can be generated by reaction of **1a** with 1.1 equiv of AgBF₄ in the presence of excess acrylonitrile with dichloromethane as solvent (eq 3). **3**



is isolated as an orange-yellow, air- and moisture-stable solid in ca. 70% yield and demonstrates solubility similar to **2a**. Lability of coordinated acrylonitrile in **3** was observed since the complex undergoes reversible exchange between acrylonitrile and acetonitrile (Scheme 2).

The ¹H NMR spectrum of complex **3** is comparable to the acetonitrile analogue (see Table 1), excluding the peaks associated with acetonitrile and acrylonitrile ligands. All resonances for coordinated acrylonitrile are shifted relative to the same resonances of the free α-olefin. Two doublets corresponding to the methylene

Scheme 2



group are centered at δ 6.27 ($^3J_{\text{HH}} = 12$ Hz) and 5.97 ($^3J_{\text{HH}} = 18$ Hz). The larger coupling constant for the latter resonance indicates that it is the proton on the β -carbon cis to the nitrile group and trans to the third olefinic proton. The α -proton of acrylonitrile appears as a doublet of doublets at δ 5.52 ($^3J_{\text{HH}} = 12$ and 18 Hz) with both cis and trans couplings to the protons of the methylene group. All of the coupling constants for free and coordinated acrylonitrile are identical.

Due to the ambidentate nature of acrylonitrile, a question arises regarding how the olefin is coordinated to the metal, i.e., through the olefin or through the nitrile. A comparison of complex **3** with other known acrylonitrile complexes reported in the literature³¹ has led to the conclusion that coordination is occurring through the nitrile group. The most compelling evidence for such an assignment is the observation of a substantial higher energy shift of ν_{CN} from 2228 to 2305 cm^{-1} upon coordination.

Synthesis of [(TIPS-6-MPD)Pt(Me)(ethylene)]-BF₄ (4**).** The synthesis of complex **4** can be achieved by reaction of **1a** and 1.1 equiv of AgBF_4 in an ethylene-saturated solution of CH_2Cl_2 (eq 3). Complex **4** is isolated as a yellow-orange solid in 75% yield and may subsequently be purified by recrystallization from CH_2Cl_2 /hexanes (1:5 v/v) at -35 $^\circ\text{C}$. The complex demonstrates solubility similar to the other cationic complexes with the exception that it is soluble in hexanes and toluene. **4** is stable in the solid state, and in solution it demonstrates slow decomposition after one month. Characterization was accomplished by ^1H and $^{13}\text{C}\{^1\text{H}\}$ NMR spectroscopies and elemental analyses.

Exchange between coordinated acetonitrile of complex **2a** and excess ethylene is an additional pathway for generation of **4** (Scheme 2), further demonstrating the lability of the coordinated donor molecules.

In the ^1H NMR spectrum, ethylene adduct **4** is similar to the other cationic complexes (Table 1). The coordinated ethylene resonance is centered at δ 3.97 ($J_{\text{Pt-H}} \approx 64$ Hz) and shifted 1.4 ppm upfield from the free olefin. This difference, i.e., $\Delta\delta$ in Hz, allows the rate of exchange between coordinated and free ethylene to be estimated as $1.2 \times 10^3 \text{ s}^{-1}$ at T_c (>363 K). As shown in Figure 2, the breadth of the coordinated ethylene resonance of **4** increases as additional ethylene is introduced into the NMR tube. The observation that the features of the resonance are dependent upon the concentration of free ethylene in solution indicates that exchange is occurring *associatively*, not dissociatively. Additional evidence for associative exchange is discussed below.

A $^{13}\text{C}\{^1\text{H}\}$ NMR spectrum was obtained of the ethylene adduct in CD_2Cl_2 and demonstrates ligand chemical shifts similar to the other cationic complexes of Table 2. Coordinated ethylene is observed as a sharp singlet at δ 77.3 with $J_{\text{Pt-C}} = 182$ Hz. Observation of only one carbon resonance for coordinated ethylene is consistent with rapid rotation of the olefin, which persists down to 193 K.

Synthesis of Cationic Platinum Complexes 5–9 via Ligand Exchange with 2a. Synthesis of [(TIPS-6-MPD)Pt(Me)(*trans*-NCCHCHCN)]BF₄ (5**).** Complex **5** was generated in a resealable NMR tube in CDCl_3 via exchange of the coordinated acetonitrile of **2a** with fumaronitrile present in excess (Scheme 2). The reaction was slow relative to the other exchange reactions

(31) Bryan, S. J.; Huggett, P. G.; Wade, K.; Daniels, J. A.; Jennings, J. R. *Coord. Chem. Rev.* **1982**, *44*, 149–189.

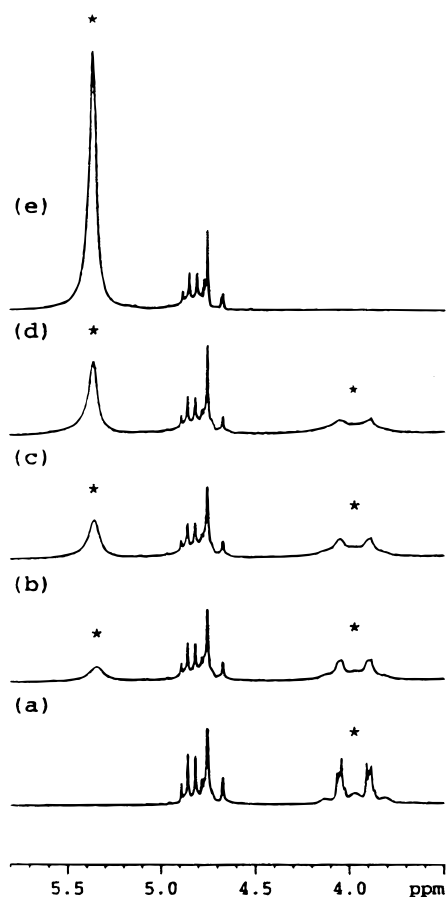


Figure 2. Section of ^1H NMR spectrum of **4**. Traces demonstrate the concentration dependence of free ethylene on the features of the coordinated ethylene resonance: (a) 0 equiv; (b) 1 equiv; (c) 2 equiv; (d) 4 equiv; (e) ethylene atmosphere. Asterisks pertain to free (5.35 ppm) and coordinated (3.97 ppm) ethylene resonances.

discussed in this paper and reached an apparent 1:1 equilibrium of **5:2a** after 1 day. Attempts at complete conversion of the acetonitrile adduct to **5** were unsuccessful. The inability of fumaronitrile to completely displace acetonitrile is possibly a result of the electron-withdrawing nature of the second nitrile substituent on the donor ability of the first.

Due to the inability of fumaronitrile to completely displace acetonitrile, exchange with the more labile ethylene ligand of complex **4** was conducted in an NMR tube. Table 1 summarizes the NMR spectral data for **5**, which are quite similar to those of the other cationic complexes. Resonances for coordinated fumaronitrile are observed as doublets at δ 6.20 and 6.07 with $^3J_{\text{trans}} = 16$ Hz compared to a singlet at δ 6.26 for the free molecule. Due to the excess fumaronitrile present in the sample, it was not possible to obtain ν_{NC} since the nitrile stretch of the free ligand obscured the coordinated ligand's stretching frequencies. On the basis of the manner of coordination demonstrated by acrylonitrile in **3**, it is believed that **5** corresponds to a single nitrile-coordinated complex.

Synthesis of [(TIPS-6-MPD)Pt(Me)(*cis*-NCCH=CH₂Et)]BF₄ (6**).** Complex **6** was generated in an NMR tube by the addition of excess *cis*-pentenenitrile to **2a**. After 10 min, the excess olefin was removed and the residue redissolved in CDCl₃. The complex was charac-

terized by ^1H NMR and IR spectroscopies. The resonances of the olefinic hydrogens are observed at δ 6.68 (β -proton) and 5.25 (α -proton, $^3J_{\text{cis}} = 11$ Hz), and the methylene and terminal methyl protons of the ethyl substituent are observed at δ 1.90 and 0.95 ($^3J_{\text{HH}} = 7.4$ Hz), respectively. As for acrylonitrile and fumaronitrile, *cis*-pentenenitrile is coordinated to Pt(II) through the nitrile and not via the olefin. Consistent with this notion, the stretch seen at 2270 cm^{-1} (ν_{CN}) for **6** is shifted 50 cm^{-1} to higher energy relative to free *cis*-pentenenitrile.

Competitive Binding Studies. To further gauge the electronic effects of the substituents on the olefin, competitive exchange reactions were conducted between the three nitriles. An equimolar mixture of acrylonitrile and fumaronitrile in CDCl₃ was added to an NMR tube containing complex **2a**. After 30 min, only resonances corresponding to **3** were observed, indicating that acrylonitrile coordinates more strongly to platinum than fumaronitrile, presumably as a result of the latter's reduced nitrile basicity.

In a second competitive binding experiment, an equimolar solution of acrylonitrile and *cis*-pentenenitrile in CDCl₃ was used. After 5 min, the acetonitrile complex had completely converted to **6**. This result demonstrates that, although acrylonitrile is less bulky than *cis*-pentenenitrile, electronic effects play a substantial role in the ligands' abilities to bind. The ethyl group of *cis*-pentenenitrile increases its ability to stabilize the cationic metal center relative to acrylonitrile.

Generation of [(TIPS-6-MPD)Pt(Me)(L)]BF₄, Where L = Benzonitrile (7**), SMe₂ (**8**), and CO (**9**).** Reversible exchange of the acetonitrile ligand of **2a** by the donor ligands benzonitrile, SMe₂, and CO was found to occur when an excess of the corresponding molecule was present in solution. Each of the complexes was characterized via ^1H NMR analysis, and the chemical shifts are recorded in Table 1. A kinetic analysis involving the exchange reaction of acetonitrile by benzonitrile is described below to provide further insight into the mechanism by which exchange occurs. Confirmation of the correct assignment of the coordinated dimethyl sulfide resonance of **8** was accomplished by conducting an exchange reaction between **8** and dimethyl sulfide-*d*₆ in the manner discussed above for the acetonitrile adduct. Additionally, the ν_{CO} stretch for **9** is observed at 2116 cm^{-1} in the IR spectrum and further corroborates the generation of this complex.

Kinetic Studies of the Concentration Dependence on the Exchange Reactions. For square-planar complexes, ligand substitution occurs associatively through a five-coordinate intermediate formed by the entering ligand binding to the metal at one of its axial sites. Brookhart has proposed that the aryl substituents hinder or significantly impede the usual substitution and metal alkyl decomposition paths, the latter via β -hydride elimination, so that polymer chain growth becomes the dominant (most rapid) kinetic process. For the complexes discussed in this report, it was initially thought that similar observations would be made regarding the ability to undergo various ligand substitution reactions. However, it was unexpectedly observed that they demonstrate relatively facile ligand exchange when qualitatively compared to the systems containing

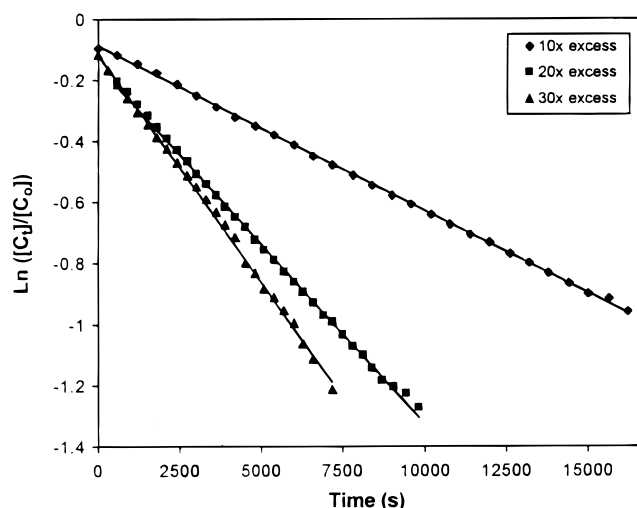


Figure 3. Kinetic analysis of the exchange reaction between complex **2a** and excess benzonitrile monitoring for disappearance of coordinated acetonitrile in the ^1H NMR spectrum. The analysis was done under pseudo-first-order conditions at 278 K.

the **MOM-4,6-DBPD** ligand. Furthermore, the results of the ethylene exchange studies with complex **4** indicated that it was undergoing exchange associatively.

A kinetics study examining the rate of ligand substitution as a function of incoming ligand concentration was conducted for acetonitrile complex **2a**. For these experiments, the concentration of **2a** in each of three NMR tubes was held constant at 0.014 M. Benzonitrile was added to each of the solutions in 10-, 20-, and 30-fold excesses at 258 K prior to the respective runs. The ligand exchange reactions were followed spectroscopically at 278 K by monitoring the appearance of free acetonitrile and disappearance of coordinated acetonitrile.³² As shown in Figure 3, the 10-, 20-, and 30-fold excesses of benzonitrile yielded first-order rate constants of $5.40(4) \times 10^{-5}$, $1.17(2) \times 10^{-4}$, and $1.49(4) \times 10^{-4} \text{ s}^{-1}$, respectively, which allowed for calculation of the second-order rate constant k_2 as $(3.2 \pm 2.0) \times 10^{-4} \text{ M}^{-1} \text{ s}^{-1}$.

While the structure of **2a** indicates that it is sterically encumbered in the axial coordination sites, space-filling models suggest that a structural reorganization can occur to accommodate the steric interactions between the TIPS groups and the incoming ligand. For example, slight rotation of the phenyl rings about the N–C(_{ipso}) bond situates the silyl-ether groups farther away from the metal, allowing bonding interactions between orbitals of the entering ligand and the metal to occur.

Polymerization of Electron-Rich Monomers. We previously communicated⁷ the observation that complex **2a** can polymerize the electron-rich olefins ethyl vinyl ether (EVE) and *N*-vinylcarbazole (NVC). Specifically, **2a** in chloroform was found to promote formation of poly-EVE with a M_w of ca. 8900 and a polydispersity of 1.7 when done at 303 K. A corresponding reaction of **2a** and *N*-vinylcarbazole yielded poly-NVC with a M_w of ca. 23 000 and M_w/M_n of 3.1. Numerous experiments were conducted probing the nature of the polymerization, the results of which were found to be consistent with generation of a stabilized carbocation that would undergo subsequent propagation and polymer formation. The following observations summarize the preliminary

work. Results of an end group analysis indicated that aldehyde formation was occurring when the reactions were worked up by doing a methanol quench and an aqueous washing. Additionally, the tacticity of the isolated polymer demonstrated a dependence upon the polarity of the solvent, specifically a decrease in isotacticity as solvent polarity was increased. The solvent dependence was larger than would be expected if the polymerization were occurring directly at the platinum center. If coordination/insertion chemistry were occurring, the quasi C_2 symmetry of complex **2a** would result in higher degrees of isotactic polymer than were observed, especially considering that completely atactic polymer was obtained for reactions conducted in the most polar solvent of the series, nitromethane. Finally, the fact that **2a** oligomerizes 2,3-dihydrofuran and not 2,5-dihydrofuran indicates that direct stabilization of the incipient carbocation by oxygen is necessary for polymerization to occur.

While the results reported in the preliminary work were consistent with cationic polymerization of the electron-rich monomers, the role of the platinum complex in initiating the polymerization was not unambiguously determined in that study. Complex **2a** may directly initiate polymerization by formation of a nonclassical sigma complex, Scheme 3a, as proposed by Baird^{33,34} in the $[\text{CpTiMe}_2][\text{BMe}(\text{C}_6\text{F}_5)_3]$ system, or by generation of an intermediate due to Lewis acid interaction of **2a** with some species present in the reaction mixture.

It has been well documented³⁵ that some Lewis acids require water as a co-initiator for the polymerization of vinyl ethers due to in situ generation of acid. Since it was not possible to completely rule out initiation by acid based on the above results, additional experiments were conducted to probe this pathway. Attempts were made at the generation of a discrete cationic aquo complex via halide abstraction from the chloro methyl precursor **1a** in the presence of water, but these led to extensive decomposition. Thus, an aquo analogue of **2a**, which could in principle serve as a possible source of H^+ , was found not to be stable at room temperature or under the reaction conditions in which the polymerizations were conducted. However, the interaction of an individual water molecule with the cationic complex **2a** leading to a Bronsted acid, Scheme 3b, could not be ruled out.

A series of experiments were conducted in the presence of base to probe whether generation of adventitious acid is responsible for initiation. The experiments described below were carried out using both EVE and NVC as the monomers. In both sets of experiments, the observations were identical. To minimize coordination of the base to complex **2a**, 2,6-di-*tert*-butylpyridine was one of the bases chosen for the experiments. Polymer formation was observed when either EVE or NVC was used, although the rate of polymerization was noticeably slower. Retardation of the rate of propagation has been reported³⁵ for other cationically initiated systems when base is present.

(32) It was determined that both of these methods resulted in identical values for the observed rate constants.

(33) Wang, Q.; Baird, M. C. *Macromolecules* **1995**, *28*, 8021–8027.

(34) Quyoum, R.; Wang, Q.; Tudoret, M.-J.; Baird, M. C.; Gillis, D. J. *J. Am. Chem. Soc.* **1994**, *116*, 6435–6436.

(35) Kennedy, J. P.; Kelen, T.; Guhaniyogi, S. C.; Chou, R. T. J. *Macromol. Sci.-Chem.* **1982**, *A18*(1), 129–152.

Scheme 3

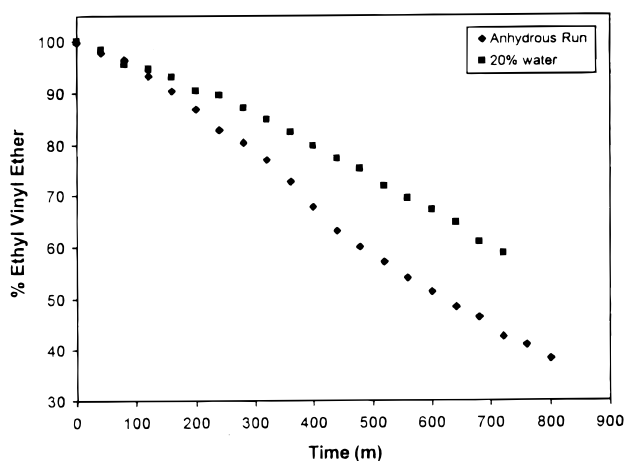
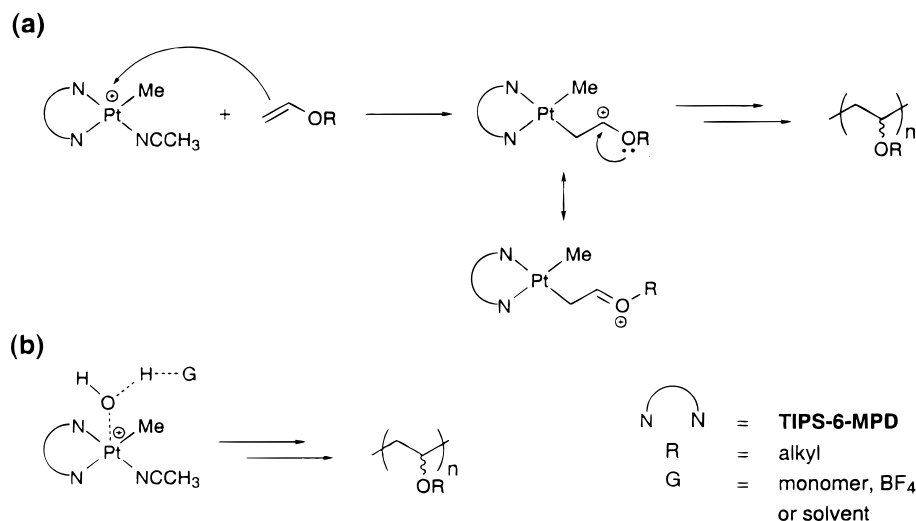


Figure 4. Influence of water on rate of ethyl vinyl ether consumption vs time. Water concentration is approximately 20% relative to complex **2a**.

Since 2,6-di-*tert*-butylpyridine had been found to affect carbocation propagation detrimentally via induced chain termination³⁶ or even coordination to the catalyst/initiator,³⁷ a second set of experiments employed a base that can be removed from the reaction mixture prior to addition of the monomer. Accordingly, a methylene chloride solution of complex **2a** was treated with the solid supported-base piperidinomethyl polystyrene for 4 h, after which the base was removed by filtration and monomer was added. Polymer formation was observed to occur with both EVE and NVC. The aforementioned experiments demonstrate that protonic impurities are not serving as the initiators for these systems in the presence of base and the rigorous absence of water.

The effect of water on the polymerization of EVE is shown in Figure 4. From the % conversion vs time plot, it is evident that water does *not* co-initiate polymerization of EVE, but rather that its presence *inhibits* polymer formation due to its reaction with the propagating carbocation.³⁸ The polymerization process eventually recovers ca. 250 min into the reaction, at which

point the rates of propagation for both of the samples with and without water are the same. These experiments are reproducible and lend further support to the notion that the platinum complex is acting as the sole initiator, Scheme 3a.

Other substrates such as styrene, α -methylstyrene, *p*-methoxystyrene, isobutylene, and (+)- β -pinene, which have been known to undergo cationically initiated polymerizations or rearrangements, were also examined using the cationic complexes. When the reaction between complex **2a** and *p*-methoxystyrene was examined, polymer was observed to form in the ¹H NMR spectrum over the period of several days at room temperature. The reaction was found to be extremely slow when compared to poly-EVE formation, even when run at 333 K. (+)- β -Pinene was observed to react slowly with complex **4**³⁹ over several days; however, the nature of the reaction was not discernible due to poor conversion and the complexity of the resulting spectrum. Attempts at increasing product formation by heating the reaction mixture led to decomposition of the platinum species in solution, as was evidenced by formation of a black solid on the walls of the NMR tube.

The lack of reactivity of these substrates may be explained by considering the relative stability of the incipient carbocation. It is well known that EVE and NVC are more active toward cationic initiators than styrene since the donating ability of the heteroatom offers the carbocation greater stability.^{40–42} In the case of α -methylstyrene, steric effects may explain the observed inactivity since coordination of this molecule was not observed to occur with either **2a** or **4**, even at elevated temperatures.

Conclusions

The silyl-protected 1,4-diazabutadiene ligands **TIPS-6-MPD** and **TIPS-4-MPD** and their subsequent coor-

(38) Biswas, M.; Kamannarayana, P. *J. Polym. Sci.: Polym. Chem. Ed.* **1976**, *14*, 2071–2077.

(39) Complex **4** was employed for this reaction since the ethylene ligand is more labile than coordinated acetonitrile. Thus, no reaction between **2a** and (+)- β -pinene was observed.

(40) Elnahas, A. M.; Clark, T. *J. Org. Chem.* **1995**, *60*, 8023–8027.
 (41) Taft, R. W.; Martin, R. H.; Lampe, F. W. *J. Am. Chem. Soc.* **1965**, *87*, 2490–2491.

(42) Sawamoto, M. *Prog. Polym. Sci.* **1991**, *16*, 111–172.

(36) Guhaniyogi, S. C.; Kennedy, J. P.; Ferry, W. M. *J. Macromol. Sci.-Chem.* **1982**, *A18(1)*, 25–37.

(37) Bennevault, V.; Peruch, F.; Deffieux, A. *Macromol. Chem. Phys.* **1996**, *197*, 2603–2613.

dination to Pt(II) have been described. Halide abstraction from the chloro methyl complexes led to the generation of a series of cationic solvent/olefin adducts that were characterized by ^1H and $^{13}\text{C}\{^1\text{H}\}$ NMR spectroscopies and elemental analyses. Exchange reactions were examined in which the acetonitrile ligand of complex **2a** was displaced reversibly by acrylonitrile, ethylene, fumaronitrile, *cis*-pentenenitrile, benzonitrile, dimethyl sulfide, and carbon monoxide to generate new cationic platinum complexes **3–9**, respectively. It was determined through a kinetic investigation of benzonitrile exchange that these substitution reactions are occurring in an associative manner. The acetonitrile complex **2a** demonstrates the extraordinary ability to induce polymer formation of various electron-rich monomers. A mechanistic analysis addressing the manner of initiation and propagation was conducted to determine the nature of the polymerization process. These studies provide evidence for direct cationic initiation by complex **2a**. Since these complexes contain weakly bound molecules, they may serve as precursors for catalysts in bond activation and polymerization processes.

Experimental Section

Materials and General Procedures. 2-Amino-3-methylbenzyl alcohol (Aldrich), 2-amino-5-methylbenzyl alcohol (Aldrich), glyoxal (Aldrich), triisopropylchlorosilane (Aldrich), AgBF_4 (Strem), *N*-vinylcarbazole (Aldrich), 2,6-di-*tert*-butylpyridine (Aldrich), and piperidinomethyl polystyrene HL (200–400 mesh, 3.48 mmol/g, NovaBiochem) were used as received. Toluene- d_6 (Cambridge Isotope), bromobenzene- d_5 (Aldrich), and nitromethane- d_3 (Aldrich) were purchased in ampules and used without further purification. Chloroform- d_1 (Cambridge Isotope) was dried over CaH_2 , freeze–pump–thawed, vacuum transferred to an oven-dried storage flask, and stored in the dark in the glovebox until use. Molecular sieves (4 Å) were activated under dynamic vacuum (0.1 mm) for 2 days at 473 K. Tetramethylsilane (Aldrich) was dried over 4 Å activated molecular sieves, freeze–pump–thawed, vacuum transferred to an oven-dried storage flask, and stored in a glovebox at 233 K. Dichloromethane- d_2 (Cambridge Isotope) was dried over 4 Å activated molecular sieves, freeze–pump–thawed, vacuum transferred to an oven-dried storage flask, and stored in the dark in the glovebox. Ethyl vinyl ether (Aldrich) was purified for the studies probing the effects of base and water on the polymerization. For those experiments, EVE was dried over KOH, freeze–pump–thawed, vacuum transferred to an oven-dried storage flask containing piperidinomethyl polystyrene, and stored in a glovebox at 233 K. Immediately before use, the olefin was filtered through a frit in the glovebox to remove the polymer-supported base. *trans*-Pt(SMe $_2$) $_2$ MeCl was synthesized according to a published procedure.⁴³

All reactions and manipulations, unless otherwise stated, were performed in dry glassware under nitrogen atmosphere using either standard Schlenk techniques or an inert-atmosphere glovebox. All NMR spectra were recorded on a Bruker AMX or a Bruker Avance 400 MHz spectrometer. ^1H and ^{13}C chemical shifts (δ in ppm) are relative to tetramethylsilane and referenced using chemical shifts of residual solvent resonances. Differential scanning calorimetric (DSC) measurements were recorded using a TA 2920 system. Gel permeation chromatography (GPC) experiments were done using a Waters Model 600E liquid chromatograph fitted with a Waters Model 996 photodiode array detector and a Waters

Model 410 differential refractometer using chloroform as eluant at room temperature. Data were analyzed using polystyrene calibration curves. Tables 1 and 2 contain the ^1H and $^{13}\text{C}\{^1\text{H}\}$ NMR data for the ligands and platinum complexes discussed in this paper. IR spectra were recorded on a 6020 Galaxy series FT-IR spectrometer. Elemental analyses were obtained from Quantitative Technologies, Inc., Whitehouse, NJ.

Synthesis of Ligands and Complexes

(2- α -Triisopropylsiloxymethyl)-6-methylaniline. A 250 mL round-bottom flask was charged with imidazole (5.88 g, 86 mmol), 2-amino-3-methylbenzyl alcohol (4.74 g, 35 mmol), 4-(dimethylamino)pyridine (0.42 g, 3.4 mmol), and 95 mL of CH_2Cl_2 . The solution was cooled to 0 °C. Triisopropylchlorosilane (10 g, 52 mmol) was added via syringe, resulting in the immediate formation of a white precipitate. The reaction mixture was warmed to room temperature and stirred overnight. It was filtered, washed with three 100 mL of portions of water and brine, and then dried over anhydrous Na_2SO_4 to give 8.9 g (88%) as a clear, pale yellow oil. Purification was not necessary for the next step. ^1H NMR (CDCl_3): δ 6.99 (d, 1H, $^3J_{\text{HH}} = 7.5$ Hz, C $_6$ H), 6.90 (d, 1H, $^3J_{\text{HH}} = 7.3$ Hz, C $_6$ H), 6.61 (t, 1H, $^3J_{\text{HH}} = 7.6$ Hz, C $_6$ H), 4.76 (s, 2H, CH $_2$), 4.30 (br s, 2H, NH $_2$), 2.17 (s, 3H, CH $_3$), 1.13 (sep, 3H, Si(CH(CH $_3$) $_2$) $_3$), 1.01 (d, 18H, $^3J_{\text{HH}} = 6.6$ Hz, Si(CH(CH $_3$) $_2$) $_3$).

(2- α -Triisopropylsiloxymethyl)-4-methylaniline. The same procedure was followed as described above for the synthesis of (2- α -triisopropylsiloxymethyl)-6-methylaniline. Imidazole (2.86 g, 42 mmol), 2-amino-5-methylbenzyl alcohol (2.34 g, 17 mmol), 4-(dimethylamino)pyridine (0.21 g, 1.7 mmol), triisopropylchlorosilane (5.5 mL, 26 mmol), and 80 mL of CH_2Cl_2 were used. Yield: 4.4 g (88%). ^1H NMR (CDCl_3): δ 6.88 (d, 1H, $J_{\text{ortho}} = 7.8$ Hz, C $_6$ H), 6.83 (s, 1H, C $_6$ H), 6.57 (d, 1H, $J_{\text{ortho}} = 7.9$ Hz, C $_6$ H), 4.71 (s, 2H, CH $_2$), 4.10 (br s, 2H, NH $_2$), 2.20 (s, 3H, CH $_3$), 1.10 (sep, 3H, Si(CH(CH $_3$) $_2$) $_3$), 1.04 (d, 18H, $^3J_{\text{HH}} = 9.0$ Hz, Si(CH(CH $_3$) $_2$) $_3$).

Glyoxal-Bis((2- α -triisopropylsiloxymethyl)-6-methylphenyl)diimine (TIPS-6-MPD). A 25 mL round-bottom flask was charged with (2- α -triisopropylsiloxymethyl)-6-methylaniline (2.15 g, 7.3 mmol), glyoxal (0.42 mL, 3.6 mmol, 40% in water), and 9 mL of absolute ethanol. The color of the reaction mixture changed from colorless to yellow almost instantaneously, and a yellow precipitate formed after a few hours. The reaction was stirred for 24 h before isolation of the product. The flask was cooled to –35 °C, and the yellow solid was collected and washed with cold methanol. The product may be purified further by recrystallization from CH_2Cl_2 /ethanol (1:5 v/v). Yield: 1.53 g (69%). Anal. Calcd for $\text{C}_{36}\text{H}_{60}\text{N}_2\text{O}_2\text{Si}_2$: C, 70.99; H, 9.93; N, 4.60. Found: C, 70.92; H, 9.63; N, 4.53.

Glyoxal-Bis((2- α -triisopropylsiloxymethyl)-4-methylphenyl)diimine (TIPS-4-MPD). The same procedure was followed as described above for the synthesis of TIPS-6-MPD. (2- α -Triisopropylsiloxymethyl)-4-methylaniline (6.96 g, 24 mmol), glyoxal (1.36 mL, 12 mmol, 40% in water), and 20 mL of absolute ethanol were used. Yield: 4.9 g (68%). Anal. Calcd for $\text{C}_{36}\text{H}_{60}\text{N}_2\text{O}_2\text{Si}_2 \cdot 1/2\text{CH}_3\text{CH}_2\text{OH}$: C, 70.31; H, 10.05; N, 4.43. Found: C, 70.38; H, 10.06; N, 4.42.

(TIPS-6-MPD)Pt(Me)Cl (1a). A 100 mL two-necked round-bottom flask was charged with *trans*-Pt(SMe $_2$) $_2$ MeCl (0.63 g, 1.7 mmol), TIPS-6-MPD (1.14 g, 1.9 mmol), and 60 mL of CH_2Cl_2 . An immediate color change from yellow to purple resulted. The flask was fitted with a gas inlet and a reflux condenser. The reaction mixture was refluxed under a slow N_2 flow overnight or until all of the platinum complex was consumed by monitoring with ^1H NMR spectroscopy. The reaction mixture was allowed to cool to room temperature, filtered, and concentrated. The oily, purple residue was thoroughly dried under vacuum. The product was triturated with hexanes and

(43) Scott, J. D.; Puddephatt, R. J. *Organometallics* **1983**, *2*, 1643–1648.

cooled to $-35\text{ }^{\circ}\text{C}$, and the purple solid was collected and washed with cold hexanes. The product may be purified by recrystallization from $\text{CH}_2\text{Cl}_2/\text{hexanes}$ (1:4 v/v). Yield: 1.33 (91%). Anal. Calcd for $\text{C}_{37}\text{H}_{63}\text{ClN}_2\text{O}_2\text{PtSi}_2$: C, 52.00; H, 7.43; N, 3.28. Found: C, 51.99; H, 7.33; N, 3.17.

(TIPS-4-MPD)Pt(Me)Cl (1b). The same procedure was followed as described above for the synthesis of **1a**. *trans*-Pt(SMe_2) $_2$ MeCl (0.79 g, 2.14 mmol), **TIPS-4-MPD** (1.45 g, 2.37 mmol), and 70 mL of CH_2Cl_2 were used. Yield: 1.19 g (65%). Anal. Calcd for $\text{C}_{37}\text{H}_{63}\text{ClN}_2\text{O}_2\text{PtSi}_2 \cdot 1/4\text{CH}_2\text{Cl}_2$: C, 51.10; H, 7.31; N, 3.20. Found: C, 51.40; H, 7.36; N, 3.18.

[(TIPS-6-MPD)Pt(Me)(CH₃CN)]BF₄ (2a). A 50 mL Schlenk flask was charged with **1a** (0.39 g, 0.46 mmol) and 30 mL of degassed acetonitrile. AgBF_4 (0.095 g, 0.49 mmol) was added as a solid under a nitrogen flow. The reaction mixture was stirred in the dark for 24 h followed by removal of the solvent in vacuo. The orange residue was redissolved in dichloromethane, and the silver salt was filtered by passing the orange solution through a frit packed with glass wool. The filtrate was then concentrated, yielding an oily, orange residue. The residue was triturated with hexanes until a fine orange-yellow solid was present and cooled to $-35\text{ }^{\circ}\text{C}$, and the product was collected and washed with cold hexanes. Complex **2a** may be recrystallized from $\text{CH}_2\text{Cl}_2/\text{hexanes}$ (1:4 v/v). Yield: 0.31 g (72%). Anal. Calcd for $\text{C}_{39}\text{H}_{66}\text{N}_3\text{O}_2\text{PtSi}_2\text{BF}_4$: C, 49.46; H, 7.02; N, 4.44. Found: C, 49.50; H, 7.06; N, 4.38.

[(TIPS-4-MPD)Pt(Me)(CH₃CN)]BF₄ (2b). The same procedure was followed as described above for the synthesis of **2a**. **1b** (0.43 g, 0.50 mmol), AgBF_4 (0.10 g, 0.51 mmol), and 30 mL of CH_3CN were used. Yield: 0.40 g (85%). Anal. Calcd for $\text{C}_{39}\text{H}_{66}\text{N}_3\text{O}_2\text{PtSi}_2\text{BF}_4$: C, 49.46; H, 7.02; N, 4.44. Found: C, 49.29; H, 7.09; N, 4.53.

Synthesis of [(TIPS-6-MPD)Pt(Me)(C₂H₃CN)]BF₄ (3). A 50 mL Schlenk flask was charged with **1a** (0.093 g, 0.11 mmol), acrylonitrile (20 μL , 0.30 mmol), and 15 mL of degassed CH_2Cl_2 . AgBF_4 (0.023 g, 0.12 mmol) was then added as a solid under a nitrogen flow. The reaction mixture was stirred in the dark for 24 h. The silver salt was filtered by passing the orange solution through Celite. The filtrate was then concentrated, yielding an oily, orange residue. The residue was triturated with hexanes until a fine orange-yellow solid was present and cooled to $-35\text{ }^{\circ}\text{C}$, and the product was collected and washed with cold hexanes. Yield: 0.075 g (72%). IR (CH_2Cl_2 , cm^{-1}): 2305 (CN), 1000–1100 (BF_4). Anal. Calcd for $\text{C}_{40}\text{H}_{67}\text{N}_3\text{O}_2\text{PtSi}_2\text{BF}_4 \cdot 1/3\text{CH}_2\text{Cl}_2$: C, 49.02; H, 6.80; N, 4.19. Found: C, 49.12; H, 6.62; N, 4.14.

Synthesis of [(TIPS-6-MPD)Pt(Me)(ethylene)]BF₄ (4). A 100 mL Schlenk flask was charged with **1a** (0.307 g, 0.36 mmol) and 30 mL of CH_2Cl_2 (ethylene saturated). AgBF_4 (0.077 g, 0.39 mmol) was then added as a solid under an ethylene flow. The reaction mixture was stirred in the dark for 24 h. The silver salt was filtered by passing the orange solution through a frit that was packed with glass wool. The filtrate was then concentrated, yielding an orange solid. Yield: 0.25 g (75%). Anal. Calcd for $\text{C}_{39}\text{H}_{67}\text{N}_2\text{O}_2\text{PtSi}_2\text{BF}_4$: C, 50.15; H, 7.23; N, 3.00. Found: C, 49.98; H, 7.19; N, 2.89.

Exchange Reactions and Kinetics Measurements

General Procedure for Exchange of CH_3CN by CD_3CN (2a-d₅), Acrylonitrile (3), and *cis*-Pentenitrile (6). An NMR tube was charged with **2a** (ca. 4 μmol) and an excess (0.5 mL) of the corresponding nitrile. After 1 h, the volatiles were removed in vacuo, the residue was redissolved in CDCl_3 , and a ^1H NMR spectrum was obtained, indicating complete replacement of CH_3CN . IR (CH_2Cl_2 , cm^{-1}) for **6**: 2270 (CN), 1000–1100 (BF_4).

General Procedure for Exchange of CH_3CN by Ethylene (4) and CO (9). To an NMR tube containing **2a** (ca. 4 μmol) was added 0.5 mL of either ethylene or CO-saturated

CDCl_3 via syringe. After 2 h, a ^1H NMR spectrum was obtained. Complete replacement of CH_3CN was evident from the ^1H NMR spectrum. Due to the presence of excess ethylene (δ 5.35, br), the resonance for coordinated ethylene of **4** was not visible. (Removal of the volatiles in vacuo followed by redissolution of the residue in CDCl_3 allowed for observation of the coordinated ethylene resonance at δ 3.97.) IR (CH_2Cl_2 , cm^{-1}) for **9**: 2116 (CO), 1000–1100 (BF_4).

Effect of Free Ethylene on the Coordinated Ethylene Resonance of 4. A resealable NMR tube was charged with **4** (2 mg, 2.1 μmol) and 0.5 mL of CDCl_3 and plugged with a rubber septum in the glovebox. The NMR tube was removed from the glovebox, and a ^1H NMR spectrum was obtained. Using a microliter syringe, 1 equiv of ethylene (ca. 52 μL based on $V = nRT/P$) was added to the NMR tube, and it was then quickly shaken. A ^1H NMR spectrum was obtained. The syringe additions were then subsequently repeated for 2 equiv and then 4 equiv of ethylene.

Generation of [(TIPS-6-MPD)Pt(Me)(fumaronitrile)]-BF₄ (5). Procedure A. Complex **5** was generated in an NMR tube and characterized by ^1H NMR spectroscopy. An NMR tube was charged with **2a** (3.5 mg, 3.70 μmol), fumaronitrile (1.5 mg, 19.2 μmol), and 0.5 mL of CDCl_3 . The reaction was monitored by ^1H NMR spectroscopy over the period of about one week. It was determined that the reaction reached an apparent equilibrium after 24 h. Attempts at complete conversion to **5** from **2a** were unsuccessful. **Procedure B.** An NMR tube was charged with **4** (3 mg, 3.21 μmol), fumaronitrile (1.3 mg, 16.7 μmol), and CDCl_3 . The reaction was monitored by ^1H NMR spectroscopy over the period of one week. Since only 61% conversion to **5** had occurred after 2 days, the solvent was removed in vacuo and the residue was redissolved in CDCl_3 . After an additional day, complete conversion to **5** had occurred. Due to excess fumaronitrile, the stretching ν_{CN} frequencies could not be determined. Attempts at converting **4** to **5** with 1 equiv of fumaronitrile were not successful.

General Procedure for Exchange of CH_3CN by Benzonitrile (7), SMe_2 (8), and SMe_2 -d₆ (8-d₆). To an NMR tube containing complex **2a** (ca. 4 μmol) in CDCl_3 was added the corresponding reagent (ca. 40 μmol). The reaction mixture was monitored via ^1H NMR analysis until complete conversion was evident. Generation of **8** and **8-d₆** was observed after 0.5 h. Displacement of CH_3CN by benzonitrile required a longer time period.

Kinetics of Ligand Substitution Reaction. For the kinetics experiments, 1,2-dimethoxyethane (DME) was used as an internal standard in 2 times excess of **2a** and was found to not react with **2a** during course of the reaction. Two stock solutions were made for the kinetics studies. Stock solution A (0.025 M **2a**): A 1 mL volumetric flask was charged with **2a** (24.1 mg, 0.025 mmol) and 1,2-dimethoxyethane (5 μL , 0.050 mmol), diluted to the mark with CDCl_3 , and plugged with a rubber septum. Stock solution B (1.9 M benzonitrile): A 5 mL volumetric flask was charged with benzonitrile (970 μL , 9.5 mmol), diluted to the mark with CDCl_3 , and plugged with a rubber septum.

10-fold Excess. A resealable, oven-dried NMR tube was charge with 250 μL of stock solution A and 167 μL of CDCl_3 in a glovebox. The NMR tube was plugged with a rubber septum, removed from the glovebox, and cooled to 258 K in an ice/ NaCl bath. A 33 μL sample from stock solution B was then added via syringe so that it slowly dripped down the wall of the NMR tube. The tube was shaken and inserted into the NMR spectrometer with the probe precooled to 278 K. Spectra were then recorded every 10 min for the duration of the experiment.

20-fold Excess. The same procedure was followed as outlined above adding 250 μL of stock solution A, 134 μL of CDCl_3 , and 66 μL of stock solution B. Spectra were recorded every 5 min for the duration of the experiment.

30-fold Excess. The same procedure was followed as outlined above adding 250 μL of stock solution A, 101 μL of CDCl_3 , and 99 μL of stock solution B. Spectra were recorded every 5 min for the duration of the experiment.

Polymerization Studies

Effect of Base on the Polymerization of EVE and NVC. Control experiments were set up in the absence of **2a** and demonstrated no polymer formation.

Complex **2a** (25.5 mg, 27 μmol) was added to a 5 mL volumetric flask in the glovebox and filled to the mark with CD_2Cl_2 . A 0.8 mL sample was withdrawn from the stock solution and added to each of two resealable NMR tubes (Set 1). 2,6-Di-*tert*-butylpyridine (5 μL , 21 μmol) was then added to both of the NMR tubes, and they were allowed to stand for 4 h at room temperature. Piperidinomethyl polystyrene (60 mg, 209 μmol) was then added to the volumetric flask that contained the remainder of the stock solution (ca. 3.4 mL). The flask was sealed and allowed to stand with occasional agitation for 4 h at room temperature. The solution was then filtered through a medium-porosity frit into an Erlenmeyer flask to remove the solid-supported base. A 0.8 mL sample of this pretreated solution was then withdrawn and added to each of two resealable NMR tubes (Set 2). NVC (20 mg, 103 μmol) was then added to an NMR tube from each of the two sets. The NMR tubes were removed from the glovebox, and the initial spectra were obtained. EVE (11 μL , 115 μmol) was then added to the other two NMR tubes from the two sets, and the initial spectra were obtained. All of the NMR tubes were then submerged in an oil bath set to 302 K, kept in the dark, and periodically analyzed over a period of 3 days.

Effect of Water on the Rate of EVE Consumption. Experiments were conducted in resealable NMR tubes in which the consumption of EVE vs time was monitored at regularly timed intervals. Tetramethylsilane was used as an internal reference in 2.5 times excess of **2a**.

Complex **2a** (8 mg, 8.4 μmol) was added to a 1 mL volumetric flask in a glovebox. The flask was then filled to the mark with dry CD_2Cl_2 . Tetramethylsilane (3 μL , 22 μmol) was then added. A 0.5 mL sample of the stock solution was withdrawn and added to each of two resealable NMR tubes. One NMR tube was stored at 233 K until use. To the other NMR tube was added EVE (10 μL , 105 μmol). It was quickly removed from the glovebox and cooled in a dewar containing liquid nitrogen. The tube was thawed, shaken, and inserted into

the NMR spectrometer with the probe preheated to 302 K. Spectra were then recorded every 40 min for the duration of the experiment. To the second NMR tube was added water (0.02 μL , 1.1 μmol). (Judging by integration, the initial spectrum contained 20% water relative to **2a**.) The same procedure was then followed as described above for the addition of EVE and for monitoring the reaction in the spectrometer.

X-ray Crystallography. Crystals of **TIPS-6-MPD** were grown from a solution of absolute ethanol and CH_2Cl_2 (4:1). A pale yellow fragment was cut from a cluster of crystals, mounted under Paratone-8277 on a glass fiber, and immediately placed in a cold stream at -80°C on the X-ray diffractometer. The X-ray intensity data were collected on a standard Siemens SMART CCD area detector system equipped with a Mo-target X-ray tube operated at 2.0 kW (50 kV, 40 mA). A total of 1321 frames of data (1.3 hemispheres) were collected using a narrow frame method with scan widths of 0.3° in ω and exposure times of 30 s/frame using a detector-to-crystal distance of 5.09 cm. The total data collection time was approximately 12 h. Frames were integrated with the Siemens SAINT program to yield a total of 5682 reflections, of which 4021 were independent ($R_{\text{int}} = 1.18\%$, $R_{\text{sig}} = 2.36\%$) and 3622 were above $2\sigma(I)$. Laue symmetry revealed a triclinic crystal system, and the final unit cell parameters (at -80°C) were determined from the least-squares refinement of three-dimensional centroids of 4986 reflections. Data were corrected for absorption with the SADABS program. The structure was solved in space group $P\bar{1}$ using direct methods and was refined employing full-matrix least-squares on F^2 (Siemens, SHELXTL, version 5.04). For a $Z = 1$, half of the molecule is in the asymmetric unit. All of the atoms were refined anisotropically, and hydrogen atoms were included in idealized positions, giving a data-to-parameter ratio of approximately 20:1. The structure refined to a goodness of fit (GOF) of 1.066 and final residuals of $R1 = 3.66\%$ ($I > 2\sigma(I)$), $wR2 = 10.45\%$ ($I > 2\sigma(I)$).

Acknowledgment. We thank the National Science Foundation (Grant CHE 97-29311) for support of this work.

Supporting Information Available: Tables of all the pertinent crystallographic information and of the spectral data for the minor isomers **1a'**, **2a'**, **3'**, **4'**, **5'**, **6'**, **7'**, **8'**, and **9'**. This material is available free of charge via the Internet at <http://pubs.acs.org>.

OM000052X